Anal. Chem. **2007,** *79,* 4957−4966

Scanning Electrochemical Microscopy. 57. SECM Tip Voltammetry at Different Substrate Potentials under Quasi-Steady-State and Steady-State Conditions

Cynthia G. Zoski,*,† Charles R. Luman,‡ José L. Fernández,§ and Allen J. Bard*,‡

Department of Chemistry and Biochemistry, New Mexico State University, Las Cruces, New Mexico 88003, Department of Chemistry and Biochemistry, The University of Texas at Austin, Austin, Texas 78712, and Facultad de Ingenieria Quimica, Santiago del Estero 2829, (3000) Santa Fe (Santa Fe), Argentina

We discuss SECM tip voltammetry, where a UME tip is held above a conductive substrate within about a tip radius and a tip voltammogram is recorded as its potential is slowly scanned while the substrate is held at a fixed potential. When the potential of the substrate is changed, the series of steady-state tip voltammograms provide information about the reactants and products. When the potential of the substrate, E_S, is set so that the reaction at the substrate is opposite to that at the tip (the usual SECM conditions), a total positive feedback (tpf) tip voltammogram is recorded. When the substrate potential is set to values where the reaction at the substrate is the same as that occurring on the tip, the tip is shielded from the species in the bulk solution. Depending upon the substrate potential, this can cause total shielding (ts) or a voltammogram that is the result of partial feedback/partial shielding (pf-ps). The result is a series of tip voltammograms that are characterized by tpf, pf-ps, or ts, depending upon E_S. Experimental tip voltammograms resulting from the reversible reduction of TCNQ and oxidation of ferrocene in MeCN are reported. These are compared with those from simulations and approximate equations developed to describe the features of the tip voltammograms generated under tpf, ts, or pf-ps conditions. The effect of the diffusion coefficient ratio on the ability of the UME tip to reach a true steady state is also addressed and possible applications, e.g., obtaining information about the reversibility of an electrochemical reaction, the product of an electrochemical reaction, the stability of that product, or the diffusion coefficients of the electroactive species, are discussed.

In scanning electrochemical microscopy (SECM),[1−3] the current through an ultramicroelectrode (UME) tip is measured when it is held or moved in a solution in the vicinity of a substrate. When the tip is held at a fixed distance from the substrate and the tip potential, E_T, is swept linearly at a constant sweep rate, a steady-state tip voltammogram can be recorded. Thus, if an oxidizing species is reduced at the tip ($O + ne \rightarrow R$) and an underlying conductive substrate is held at a sufficiently positive potential, E_S, the R generated at the tip is oxidized back to O at the substrate. Such tip voltammograms exhibit positive feedback currents (i.e., currents greater than the diffusion-limited current, $i_{T,\infty}$, recorded at distances far from the substrate) at tip potentials where R is generated. Tip voltammograms recorded in this way have been used to study heterogeneous and homogeneous kinetics by monitoring the tip voltammogram as the distance between the tip and substrate is changed. If a similar experiment is performed over an insulator, where no oxidation of R occurs, the tip voltammogram is characterized as showing so-called "negative feedback" currents (i.e., less than $i_{T,\infty}$). When the substrate is held at a potential where the same reaction as on the tip, reduction of O to R, also occurs on the substrate, the measured tip current is even smaller than the insulator case, since the substrate consumes O and hence the tip is "shielded" from O diffusing to it from the bulk solution.[4] Under these conditions, the substrate "shields" the tip from the bulk solution. Moreover, when the tip is within a distance of approximately one tip diameter from the substrate, the tip diffusion layer interacts with the small portion of the substrate diffusion layer beneath the tip. This interaction of concentration profiles causes the reaction at that portion of the substrate underneath the approaching tip to change from $O \rightarrow R$ to $R \rightarrow O$ and positive feedback to occur even when the substrate potential is set so that the overall reaction is still $O \rightarrow R$.

We report here a series of SECM experiments in which the tip is held less than a tip diameter away from a large substrate, which is held for a length of time, a so-called quiet time, at E_S values ranging from extremely positive to extremely negative relative to the standard potential E^0. During this quiet time, a diffusion layer is established at the substrate surface correspond-

---

* To whom correspondence should be addressed. E-mail: ajbard@utexas.edu (A.J.B.); czoski@nmsu.edu (C.G.Z.).

† New Mexico State University.

‡ The University of Texas at Austin.

§ Facultad de Ingenieria Quimica.

(1) *Scanning Electrochemical Microscopy*; Bard, A. J., Mirkin, M. V., Eds.; Marcel Dekker: New York, 2001.

(2) Sun, P.; Laforge, F. O.; Mirkin, M. V. *Phys. Chem. Chem. Phys.* **2007**, *9*, 802.

(3) Fan, F.-R. R.; Fernandez, J.; Liu, B.; Mauzeroll, J. In *Handbook of Electrochemistry*; Zoski, C. G., Ed.; Elsevier: Amsterdam 2007; p 471.

(4) Zoski, C. G.; Aguilar, J. C.; Bard, A. J. *Anal. Chem.* **2003**, *75*, 2959.

10.1021/ac070021c CCC: $37.00

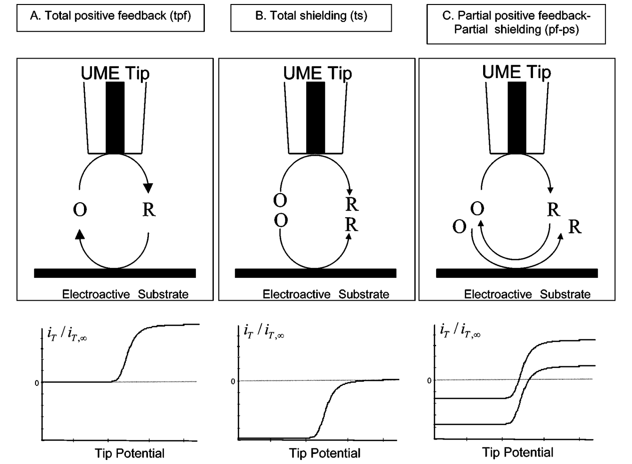

Figure 1. Schematic diagram of different SECM cases and the resulting voltammograms. (A) Total positive feedback; (B) total shielding; (C) partial feedback//partial shielding.

ing to the E_S relative to E^0 and extending a distance $(2Dt)^{1/2}$ from the substrate surface into the bulk solution[5] with the tip held at an initial potential. After the quiet time, the tip potential, E_T, is swept at a constant sweep rate to a final potential, and a tip voltammogram is recorded for each E_S. At a very positive E_S relative to E^0, there is no reduction of O at the substrate, and positive feedback occurs along the entire tip voltammogram which begins at zero current and rises to a limiting total positive feedback (tpf) current value as E_T is swept from a positive to a negative value (Figure 1A). As E_S is made increasingly negative relative to E^0, O is partially reduced at the substrate and the substrate is said to partially shield the tip from the bulk solution (Figure 1C). In this partial feedback/partial shielding (pf-ps) case, the tip voltammogram is displaced in an anodic current direction from the total positive feedback one. At a very negative E_S relative to E^0, reduction of O at the substrate occurs such that the tip is totally shielded from the bulk solution. The tip voltammogram under this total shielding (ts) condition is completely displaced from the tpf voltammogram (Figure 1B). In this situation, the substrate generated R, which the tip now sees as a bulk solution, can be oxidized to O at positive tip potentials relative to E^0.

The shielding tip voltammograms that are seen with the SECM are analogous to those found with other two-electrode electrochemical systems, such as the rotating ring–disk electrode (RRDE), interdigitated arrays (IDAs), and thin-layer cells. The current at the ring electrode, for the RRDE, decreases when the disk is placed at a potential where the same reaction is occurring.[6,7] Since the convection flow occurs totally from the disk to the ring where collection occurs, the transition to the equivalent of SECM positive feedback does not occur. Shielding and positive feedback are also found with IDAs[8] and thin-layer cells.[9–13] To our knowledge, shielding experiments of the type described here for the SECM have not been reported.

EXPERIMENTAL SECTION

Chemicals. Ferrocene (Fc; Aldrich), 7,7,8,8-tetracyanoquinodimethane (TCNQ; Aldrich), lithium perchlorate (Aldrich), sodium perchlorate monohydrate (Fluka), and tetrathiofulvalene (TTF; Fluka) were used as received. Tetra-*n*-butylammonium perchlorate (TBAP; Alfa Aesar) was recrystallized and dried under vacuum prior to use. Acetonitrile (MeCN, Fisher, HPLC grade) was stored over neutral activated alumina (MP Biomedicals Super 1). Deionized water was obtained from a Milli-Q (Millipore) deionizing system.

Electrodes. The UME tip electrode used in all experiments was fabricated by sealing a 25-μm-diameter platinum wire (Goodfellow) in a borosilicate glass capillary, polishing to yield a flat disk, and then sharpening the glass sheath to obtain an RG = 5. A 2-mm-diameter inlaid platinum disk (CH Instruments) was used as a substrate electrode, and a 0.5-mm platinum wire was used as a counter electrode. Tip and substrate electrodes were polished with 0.05-μm alumina (Buehler) prior to use. A silver quasi-reference electrode was used in all experiments and calibrated against a saturated, aqueous silver/silver chloride reference electrode (RG-5B, Bioanalytical Systems) that was isolated from the solution through a 1.0 M sodium perchlorate salt bridge. All potentials are reported with respect to this Ag/AgCl reference electrode.

SECM Investigations. A CH Instruments scanning electrochemical microscope (CHI 900, CH Instruments) was used in all experiments. The UME tip was positioned at a constant distance above the substrate by recording a positive feedback approach curve for each redox mediator and comparing to established theory for RG = 5 from which the tip/substrate distance L could be calculated.[1–3] For Fc, the UME tip potential, $E_T = 0.5$ V and the substrate potential, $E_S = 0$ V; for TCNQ, $E_T = 0$ V and $E_S = 0.5$ V. After a 5-s quiet time, a series of UME tip SECM linear sweep voltammograms (LSVs) were recorded by scanning E_T at 50 mV/s over a potential range of approximately $E_{1/2} \pm 0.25$ V. Substrate potentials E_S were varied at discrete values over the same range, and one tip SECM LSV was recorded for each E_S and normalized with respect to the absolute value of $i_{T,\infty}^{\lim}$, the diffusion-limiting UME tip current recorded at an infinite distance from the substrate.

RESULTS AND DISCUSSION

TCNQ/TCNQ$^-$. The TCNQ system is an example where the D values of reactant and product are about the same. Figure 2 shows a series of tip voltammograms (solid lines) recorded in 0.67 mM TCNQ/0.10 M TBAP in MeCN at a 12.5-μm-radius inlaid Pt disk with glass shielding corresponding to RG = 5. Substrate potential E_S ranged from 0.500 to 0 V and E_T was swept linearly at 50 mV/s. TCNQ undergoes a reversible one-electron reduction to TCNQ$^-$ in MeCN where diffusion coefficients $D_{TCNQ} = 1.44 \times 10^{-5}$ cm^2/s and $D_{TCNQ-} = 1.35 \times 10^{-5}$ cm^2/s corresponding to a ratio $D_{TCNQ}/D_{TCNQ-} = 1.07$[14] and $D_{TCNQ} = 1.8 \times 10^{-5}$ cm^2/s[15] have

---

(5) Bard, A. J.; Faulkner, L. R. *Electrochemical Methods*; Wiley: New York, 2001; pp 147, 164.

(6) Reference 5, p 352.

(7) Albery, W. J.; Hitchman, M. L. *Ring-Disk Electrodes*; Clarendon: Oxford, 1971; p 24.

(8) Bard, A. J.; Crayston, J. A.; Kittlesen, G. P.; Varco Shea, T.; Wrighton, M. S. *Anal. Chem.* **1986**, *58*, 2321.

(9) Hubbard, A. T.; Anson, F. C. In *Electroanalytical Chemistry;* Bard, A. J., Ed.; Dekker: New York, 1970; Vol. 4, p 512.

(10) Anderson, L. B.; Reilley, C. N. *J. Electroanal. Chem.* **1965**, *10*, 295.

(11) Anderson, L. B.; Reilley, C. N. *J. Electroanal. Chem.* **1965**, *10*, 538.

(12) Anderson, L. B.; McDuffie, B.; Reilley, C. N. *J. Electroanal. Chem.* **1966**, *12*, 477.

(13) Reilley, C. N. *Rev. Pure Appl. Chem.* **1968**, *18*, 137.

(14) Rongfeng, Z.; Evans, D. *J. Electroanal. Chem.* **1995**, *385*, 201.

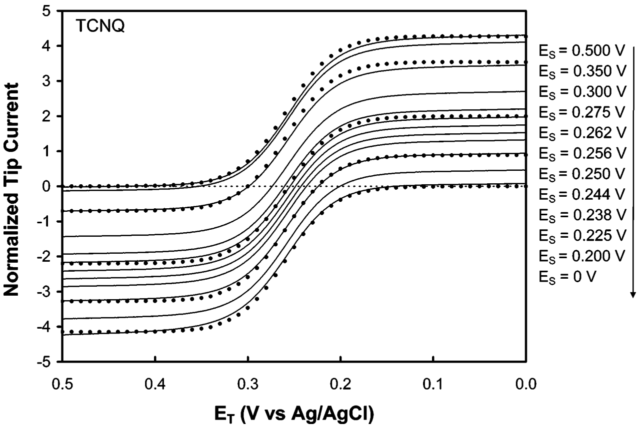

Figure 2. Tip voltammograms of 0.67 mM TCNQ/0.1 M TBAP in CH_3CN at d = 2.6 μm (L = 0.21) from a Pt substrate surface. Substrate potentials E_S correspond to tip voltammograms from top (E_S = 0.500 V) to bottom (E_S = 0 V). Solid lines indicate experimental data recorded after a 5-s quiet time and with the tip potential E_T sweeping from 0.50 to 0 V at 50 mV/s. Solid dots indicate simulated data (Femlab) with simulation parameters E_S = 0.500, 0.300, 0.256, 0.225, and 0 V, E^0 = 0.260 V, L = 0.21, $D_{TCNQ} = 1.44 \times 10^{-5}$ cm^2/s, and $D_{TCNQ^-} = 1.36 \times 10^{-5}$ cm^2/s (i.e., $D_{TCNQ}/D_{TCNQ^-} = 1.06$). Dashed line indicates zero current.

been reported. In comparison, we found $D_{TCNQ} = 2.58 \times 10^{-5}$ cm^2/s from the $i_{T,\infty}^{\lim}$current of the steady-state CV and $D_{TCNQ} = 2.34 \times 10^{-5}$ cm^2/s from the $i_{T,\infty}^{\lim}$current value measured from an approach curve at 82 μm from the substrate surface. From the $E_{1/2}$ point on a steady-state voltammogram recorded in bulk solution at a distance far from the substrate surface, we estimated a E^0 value of 0.260 V.

The UME tip was then positioned 2.6 μm above a 2-mm-diameter Pt inlaid disk substrate (corresponding to a normalized distance $L = d/a = 0.21$). During the 5-s quiet time, an equilibrium concentration profile of TCNQ/TCNQ$^-$ that is approximately $(2Dt)^{1/2}$ = 0.012 cm thick[4] is established across the substrate surface as E_S is made progressively more negative relative to $E^0 \approx 0.260$ V for each tip voltammogram. At L = 0.21, the tip is located well within this diffusion layer. As E_T is changed linearly from an initial value of 0.500 V to a final value of 0 V, the tip samples the concentrations of TCNQ and TCNQ$^-$ established at each E_S in the tip−substrate gap. We began with E_S values significantly positive of E^0 and made E_S progressively negative relative to E^0.

We first describe the resulting tip voltammograms qualitatively and then in more detail using results from following theoretical sections. At E_S = 0.500 V, only TCNQ is initially present in the tip−substrate gap. As E_T is changed linearly from 0.500 to 0 V, any TCNQ$^-$ generated at the tip is oxidized back to TCNQ at the more positive substrate and positive feedback to the tip results. Thus, the normalized cathodic tip current is initially zero at E_T = 0.500 V and increases to a limiting current value larger than $i_{T,\infty}^{\lim}$ as E_T approaches 0 V. This is the usual total positive feedback (tpf) situation normally encountered in SECM. In contrast, at E_S = 0 V, a concentration profile of TCNQ$^-$ is established across the substrate and in the tip−substrate gap during the quiet time. At the start of the scan, the tip finds itself in a solution of TCNQ$^-$. Oxidation of TCNQ$^-$ occurs at the tip as E_T is swept linearly from 0.500 to 0 V relative to E^0 with corresponding positive feedback as TCNQ$^-$ is regenerated at the underlying region of the more negative substrate. The normalized tip current begins at an anodic limiting value and ultimately reaches zero current as E_T approaches its final 0 V value. The decrease of the cathodic tip current relative to $i_{T,\infty}$ indicates that the tip is totally shielded from the bulk TCNQ solution by the reaction at the substrate. However, when the tip is at more positive potentials there is also a positive feedback of the substrate-generated TCNQ$^-$ in the gap as it is oxidized to TCNQ at the tip. This represents total shielding (ts) of the tip with respect to the bulk solution (although there is positive feedback with respect to the substrate-generated species TCNQ$^-$). In this case, the anodic limiting tip current at E_S = 0 V is approximately equal in magnitude but opposite in sign to the cathodic limiting tip current at E_S = 0.500 V since $D_{TCNQ} \approx D_{TCNQ^-}$.

As E_S is decreased in increments between the 0.500 (tpf) and 0 V (ts) limits, concentration profiles of both TCNQ and TCNQ$^-$, which depend on D_{TCNQ} and D_{TCNQ^-}, are established across the surface of the substrate and within the tip−substrate gap. At the tip, oxidation of TCNQ$^-$ occurs when E_T is well positive of E^0 and reduction of TCNQ occurs at E_T significantly more negative than E^0. Thus, the nature of the concentration profiles in the gap region and the tip current will also depend on the experimentally controlled parameters E_S, E_T, and L for a fixed quiet time. The potential, $E_T(i_T{=}0)$, where the tip voltammogram crosses zero current corresponds to total shielding of the tip by the substrate without feedback and occurs when $E_T = E_S$; this corresponds to the point where the substrate determines the concentration ratio in the gap and the concentration profiles are flat at steady state. For the tip voltammograms shown in Figure 2, E_T (i_T=0) = E_S ± 2 mV. Additionally, as E_S decreases from 0.500 to 0 V, the anodic limiting current increases while the cathodic limiting current decreases in magnitude and the entire tip voltammogram is anodically offset in current from the tpf voltammogram at E_S = 0.500 V toward the ts tip voltammogram at E_S = 0 V without a change in wave shape, as indicated by a constant half-wave potential of $E_{1/2} = 257 \pm 2$ mV. When $E_S = E^0$, one expects that the ratio of the cathodic and anodic limiting currents of a tip voltammogram will be equal to unity for equal D. In the tip voltammograms shown in Figure 2, this occurs in the vicinity of E_S = 0.256 and 0.262 V. When $E_S = E^0$, one also expects that the ratio of the cathodic limiting currents at E_S and E_S = 0.500 V(tpf), and that of the anodic limiting current at E_S and E_S = 0 V (ts), will be close to $^1/_2$ (and equal to $^1/_2$ for equal D); these criteria are met when E_S = 0.256 and 0.262 V. Thus, from the tip voltammograms shown in Figure 2, one can estimate that E^0 for the TCNQ reduction lies between 0.256 and 0.262 V, in close agreement with the 0.260 V value determined from the UME steady-state voltammogram recorded in the bulk solution.

Comparison of the experimental tip voltammograms with simulated quasi-steady-state voltammograms (solid dots, by Femlab, as described below) is shown in Figure 2 for E_S values of 0.500, 0.300, 0.256, 0.225, and 0 V. In selecting parameters in the simulation for fitting the experimental tip voltammograms, we began with the tip voltammogram corresponding to E_S = 0.500 V (tpf) where, because the normalized tip current (with $i_{T,\infty}^{\lim}$) is

---

(15) Norton, J. D.; Benson, W. E.; White, H. S.; Pendley, B. D.; Abruna, H. D. *Anal. Chem.* **1991**, *63*, 1901.

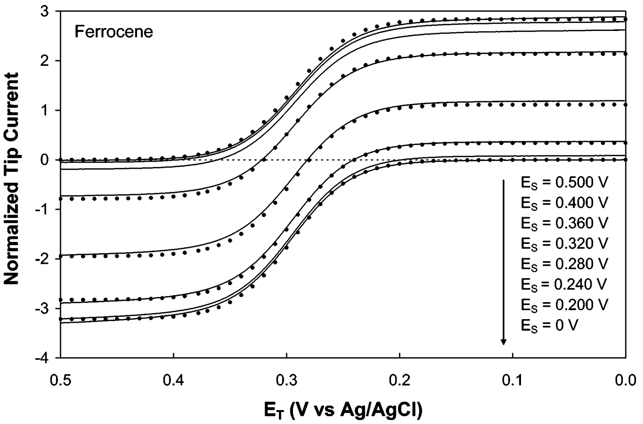

Figure 3. Tip voltammograms of 0.34 mM Fc/0.1 M TBAP in CH_3-CN at $d = 3.8$ μm ($L = 0.30$) from a Pt substrate surface. Substrate potentials E_S correspond to tip voltammograms from top ($E_S = 0.500$ V) to bottom ($E_S = 0$ V). Solid lines indicate experimental data recorded after a 5-s quiet time and with the tip potential E_T sweeping from 0 to 0.50 V at 50 mV/s. Solid dots indicate simulated data (Femlab) with simulation parameters $E_S = 0.50$, 0.32, 0.28, 0.24, and 0 V, $E^0 = 0.288$ V, $L = 0.3$, $D_{Fc+} = 1.68 \times 10^{-5}$ cm^2/s, and $D_{Fc} = 2.15 \times 10^{-5}$ cm^2/s (i.e., $D_{Fc+}/D_{Fc} = 0.78$). Dashed line indicates zero current.

independent of D_{TCNQ} and D_{TCNQ^-}, it can be used to find the normalized distance, *L*. The best fit was found for $L = 0.21$, in agreement with the value determined from the experimental approach curve. The tip voltammogram recorded at $E_S = 0$ V (ts) at the determined *L* value showed the greatest sensitivity to D_{TCNQ} and D_{TCNQ^-} values; the best fit was found when the ratio $D_{TCNQ}/D_{TCNQ^-} = 1.06$, in good agreement with the reported value of 1.07.[14] The E^0 value was then determined by fitting the tip voltammogram where $E_S = E^0$, or very close to it. The best fit for the tip voltammogram at $E_S = 0.256$ V was found to be $E^0 = 0.260$ mV. From the relationship between E^0 and $E_{1/2}$ ($E^0 = E_{1/2} + (RT/nF)\ln(D_O/D_R)$)[16] and using the experimental $E_{1/2}$ value, one calculates $E^0 = 258 \pm 3$ mV, which is in good agreement with the E^0 used in the simulations.

Fc/Fc$^+$. Ferrocene, which undergoes a reversible one-electron oxidation to the ferricinium cation Fc$^+$, is an example of a system where the *D* values of the redox couple are substantially different from each other: $D_{Fc} = 2.15 \times 10^{-5}$ cm^2/s while that for $D_{Fc+} = 1.72 \times 10^{-5}$ cm^2/s, or $D_{Fc+}/D_{Fc} = 0.80$.[17,18] In comparison, $D_{Fc} = 2.83 \times 10^{-5}$ cm^2/s was determined from tip current approach data in these experiments starting at 66 μm from the substrate where $i_T \approx i_{T,\infty}^{\lim}$. Tip voltammograms (solid lines) are shown in Figure 3 and were recorded in a 0.34 mM Fc solution (0.1 M TBAP/MeCN) at a tip−substrate separation of 3.8 μm ($L = 0.30$), at E_S ranging from 0 to 0.500 V, and E_T changing linearly from 0 to 0.500 V at 50 mV/s. The change in the concentration profiles in the tip−substrate gap and the resulting tip voltammograms with E_S follows arguments similar to those given for TCNQ. For the ferrocene case, however, the limiting tpf ($E_S = 0$ V) current is clearly larger than the limiting ts ($E_S = 0.5$ V) current, indicating that $D_{Fc} > D_{Fc+}$ as reported.[17,18] The tip potential corresponding to a zero tip current, E_T ($I_T = 0$) $\approx E_S \pm 3$ mV; this is where total shielding occurs without feedback. The tip half-wave potential was $E_{T,1/2} \approx 294 \pm 3$ mV indicating that the shape of the tip voltammograms does not change with E_S.

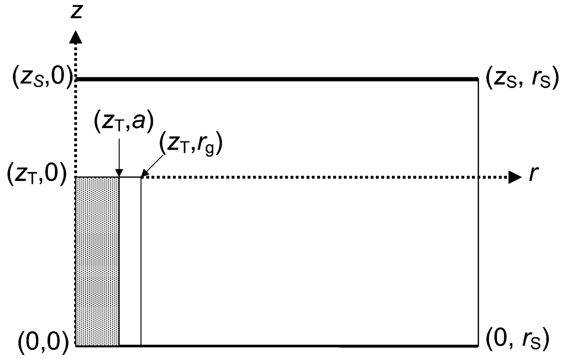

Figure 4. Schematic for SECM geometry in Femlab.

Simulated tip voltammograms (solid dots, Femlab) in Figure 3 at $E_S = 0.500$, 0.320, 0.280, 0.240, and 0 V are shown for comparison with the experimental curves. In fitting the experimental tip voltammograms, we began with the tip voltammogram corresponding to $E_S = 0$ V (tpf), which is independent of diffusion coefficients and thus can be used to set the normalized distance, *L*; the best fit was found to be $L = 0.3$ in agreement with the value determined from the experimental approach curve. The tip voltammogram recorded at $E_S = 0.5$ V (ts) at the determined *L* value showed the greatest sensitivity to the D_{Fc+}/D_{Fc} ratio; the best fit was found to be $D_{Fc+}/D_{Fc} = 0.78$, in close agreement with the previously reported value of 0.80.[17,18] The E^0 value was then determined by fitting the tip voltammogram where $E_S = E^0$, or very close to it. The best fit for the tip voltammogram at $E_S = 0.280$ V was $E^0 = 0.288$ mV. From the relationship between E^0 and $E_{1/2}$ ($E^0 = E_{1/2} + (RT/nF)\ln(D_O/D_R)$) and using the experimental $E_{1/2}$ value, one calculates $E^0 = 288 \pm 3$ mV, which is in good agreement with the E^0 used in the simulations.

Simulations: The Model. Simulations were performed using two independent methods: the COMSOL Multiphysics (Femlab, version 3.2b) finite element package with the Chemical Engineering Module in the axi-symmetric 2D mode and a 2D finite difference method written in cylindrical coordinates. The diffusion equations and boundary conditions used in the Femlab package are presented here while the details of the 2D finite difference method are reported in the Supporting Information. Both transient and steady-state Femlab simulations were performed and are discussed below.

Figure 4 shows the schematic for the SECM geometry. The time-dependent diffusion equations for species O and R are

$$\frac{\partial C_i}{\partial t} = D_i\left(\frac{\partial^2 C_i}{\partial r^2} + \frac{1}{r}\frac{\partial C_i}{\partial r} + \frac{\partial^2 C_i}{\partial z^2}\right) \tag{1}$$

where *r* and *z* are the coordinates in the directions radial and normal to the electrode surface, D_i and C_i are the diffusion coefficients and concentrations of species *i* (O or R), and *t* is time. Under steady-state conditions, the left-hand side of eq 1 is set to zero.

The model described here represents a generic SECM experiment with a disk UME tip. Initially, the solution contains either

---

(16) Reference 5, p 183.

(17) Martin, R. D.; Unwin, P. R. *Anal. Chem.* **1998**, *70*, 276.

(18) Martin, R. D.; Unwin, P. R. *J. Electroanal. Chem.* **1997**, *439*, 123.

mediator O (in the TCNQ experiments) or R (in the ferrocene experiments) at bulk concentrations C_{O}^* and C_{R}^* respectively. The reaction

$$\mathrm{O} + n\mathrm{e}^- \leftrightarrows \mathrm{R} \qquad (2)$$

is reversible and can occur on both the UME tip and the substrate. The steady-state diffusion limiting tip current at infinite distance from the substrate $i_{\mathrm{T},\infty}^{\mathrm{lim}}$ is defined by eq 3 or by eq 4 depending on whether the mediator in the bulk solution is O or R initially:

$$i_{\mathrm{T},\infty}^{\mathrm{lim},c} = \mathrm{RG_{fac}}nFD_{\mathrm{O}}C_{\mathrm{O}}^*a \quad \text{only species O in bulk solution initially} \qquad (3)$$

$$i_{\mathrm{T},\infty}^{\mathrm{lim},a} = -\mathrm{RG_{fac}}nFD_{\mathrm{R}}C_{\mathrm{R}}^*a \quad \text{only species R in bulk solution initially} \qquad (4)$$

D_{O} and D_{R} are the diffusion coefficients of O and R, respectively, a is the UME disk radius, and F is the Faraday constant. RG refers to the dimensions of the glass shielding surrounding the inlaid disk and is given by the ratio of the diameter of the glass shielding to the diameter of the inlaid conducting metal surface (i.e., RG = r_g/a, where r_g is the tip radius).[19–21] This RG value affects the steady-state limiting current, which shows up as a constant multiplier that we call here $\mathrm{RG_{fac}}$. For example, an inlaid disk electrode with an infinite glass shield (RG = ∞) has an $\mathrm{RG_{fac}} = 4$. In the experiments reported here where RG = 5, $\mathrm{RG_{fac}} = 4.144$ and was used in normalizing simulated currents.[22]

The tip is positioned at a constant distance d $(=z_{\mathrm{S}} - z_{\mathrm{T}})$ from the substrate and E_{T} is held at a value of ~0.25 V more positive (when the mediator is O), or more negative (when the mediator is R), than E^0 of reaction 2 during a quiet time period τ. After this quiet time, the tip potential is linearly scanned in a cathodic, or anodic, direction at a fixed scan rate v, until a tip potential value of ~0.25 V more negative for mediator O (or more positive for mediator R) than E^0 is reached. E_{S} is held at a constant value in the approximate range $-0.25\ \mathrm{V} < (E_{\mathrm{S}} - E^0) < 0.25\ \mathrm{V}$ during the quiet time and scan. The model is general and permits SECM phenomena such as kinetics, feedback, and shielding or a combination of these to be considered with no restrictions placed on D_{O} or D_{R}.

The initial and boundary conditions to solve this model are summarized in the Supporting Information for the cylindrical coordinate system defined in Figure 4. In the treatment here, we consider only Nernstian conditions, so $k°$, the standard rate constant, is taken as 10 cm/s. The normalized tip current ($I_{\mathrm{T}} = i_{\mathrm{T}}/|i_{\mathrm{T},\infty}^{\mathrm{lim}}|$) is

$$I_{\mathrm{T}}(t) = \frac{2\pi \int_0^a j_{\mathrm{T}}(z_{\mathrm{T}},r,t)r\,\mathrm{d}r}{|i_{\mathrm{T},\infty}^{\mathrm{lim}}|} \qquad (5)$$

where $i_{\mathrm{T},\infty}^{\mathrm{lim}}$ is given by eq 3 or 4.

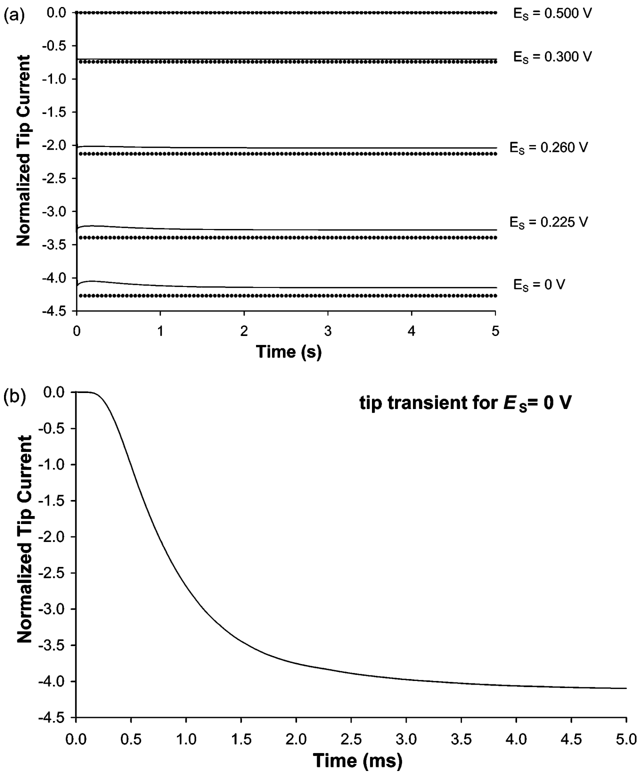

Figure 5. (a) Simulated (Femlab) transient tip response during the 5-s quiet time assuming equal (solid dots) and unequal (solid lines) diffusion coefficients for TCNQ. For equal diffusion coefficients, $D_{\mathrm{TCNQ}} = D_{\mathrm{TCNQ}^-} = 1.44 \times 10^{-5}$ cm^2/s. For unequal diffusion coefficients, $D_{\mathrm{TCNQ}} = 1.44 \times 10^{-5}$ cm^2/s and $D_{\mathrm{TCNQ}^-} = 1.36 \times 10^{-5}$ cm^2/s (i.e., $D_{\mathrm{TCNQ}}/D_{\mathrm{TCNQ}^-} = 1.06$). The tip potential E_{T} was held at 0.5 V at each of the substrate potentials E_{S}. Other parameters include $L = 0.21$ and $E^0 = 0.260$ V. (b) Short-time transient, with $D_{\mathrm{TCNQ}} = 1.44 \times 10^{-5}$ cm^2/s and $D_{\mathrm{TCNQ}^-} = 1.36 \times 10^{-5}$ cm^2/s, of the $E_{\mathrm{S}} = 0$ V transient shown in (a).

Simulations: TCNQ (Quiet Time). The tip response during the 5-s quiet time used experimentally was simulated (Femlab) by assuming either equal or unequal diffusion coefficients. For equal diffusion coefficients, we used $D_{\mathrm{TCNQ}} = D_{\mathrm{TCNQ}^-} = 1.44 \times 10^{-5}$ cm^2/s (i.e., $D_{\mathrm{TCNQ}}/D_{\mathrm{TCNQ}^-} = 1.00$), while for unequal diffusion coefficient simulations, $D_{\mathrm{TCNQ}} = 1.44 \times 10^{-5}$ cm^2/s and $D_{\mathrm{TCNQ}^-} = 1.36 \times 10^{-5}$ cm^2/s (i.e., $D_{\mathrm{TCNQ}}/D_{\mathrm{TCNQ}^-} = 1.06$). The standard potential $E^0 = 0.260$ V was used in all simulations. Figure 5 shows the normalized simulated tip current versus time response for $D_{\mathrm{TCNQ}} = D_{\mathrm{TCNQ}^-}$ (solid dots) and $D_{\mathrm{TCNQ}} \neq D_{\mathrm{TCNQ}^-}$ (solid line) at a 12.5-μm-radius (RG = 5) UME tip positioned at $L = 0.21$ above an infinite substrate. The tip was held at a constant potential $E_{\mathrm{T}} = 0.5$ V while that of the substrate was switched from open circuit to different E_{S} values in the range 0.500−0 V. When $E_{\mathrm{T}} = E_{\mathrm{S}} = 0.500$ V, there is no reaction at either the tip or substrate, and the normalized tip current is 0 throughout the quiet time. As E_{S} decreases, an anodic tip current flows in response to the TCNQ$^-$ generated in the tip−substrate gap. This tip current is initially transient in nature in that there is an anodic current flow when the TCNQ$^-$ generated at the substrate reaches the tip (in a time of the order of 2.4 ms, the so-called transit time) followed by a brief decay in the anodic current, and then an increase in the anodic current toward a steady value as the TCNQ$^-$ diffusion layer is established across the substrate and in the tip−substrate gap. Figure 5b shows the short-time transient for the $E_{\mathrm{S}} = 0$ V ts case

---

(19) Reference 1, Chapter 5.
(20) Amphlett, J. L.; Denuault, G. *J. Phys. Chem. B* **1998**, *102*, 9946.
(21) Zoski, C. G.; Liu, B.; Bard, A. J. *Anal. Chem.* **2004**, *76*, 3646.
(22) Zoski, C. G.; Mirkin, M. V. *Anal. Chem.* **2002**, *74*, 1986.

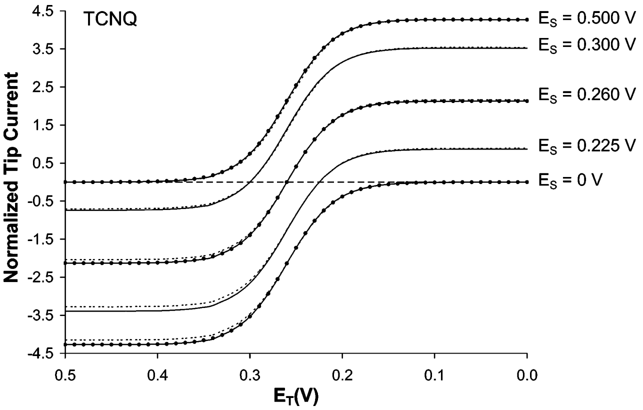

Figure 6. Comparison of quasi-steady-state (solid and dashed lines) and steady-state (solid dots) simulations (Femlab) for TCNQ. Solid lines indicate $D_{\text{TCNQ}} = D_{\text{TCNQ}^-} = 1.44 \times 10^{-5}$ cm^2/s; dashed lines indicate $D_{\text{TCNQ}} = 1.44 \times 10^{-5}$ cm^2/s and $D_{\text{TCNQ}^-} = 1.36 \times 10^{-5}$ cm^2/s (i.e., $D_{\text{TCNQ}}/D_{\text{TCNQ}^-} = 1.06$). All other simulation parameters as in Figure 2. Long-dashed line indicates zero current.

where the tip current is zero until ~0.25 ms when it begins to increase anodically. Thus, the substrate-generated TCNQ$^-$ appears to arrive at the tip much sooner than the calculated 2.4-ms transit time based on random-walk diffusion.[5] The transient nature of the tip current for a specific L is D and E_S dependent and is most apparent when $D_{\text{TCNQ}} \neq D_{\text{TCNQ}^-}$ (solid lines), and E_S is held at values equal to or more negative than E^0. For reversible conditions where $D_{\text{TCNQ}} = D_{\text{TCNQ}^-}$, and any substrate potential, the tip current (solid dots) immediately reaches a constant value that corresponds to a steady-state value which is larger in magnitude than the quasi-steady-state value observed when $D_{\text{TCNQ}} \neq D_{\text{TCNQ}^-}$. The difference between the normalized tip currents when $D_{\text{TCNQ}} = D_{\text{TCNQ}^-}$ and $D_{\text{TCNQ}} \neq D_{\text{TCNQ}^-}$ increases as the tip is increasingly shielded from the bulk solution by the substrate (i.e., as E_S decreases from 0.500 to 0 V) and the tip current gets larger. With much longer quiet times, the quasi-steady tip current value observed when $D_{\text{TCNQ}} \neq D_{\text{TCNQ}^-}$ will eventually reach the steady-state value observed for $D_{\text{TCNQ}} = D_{\text{TCNQ}^-}$ as reported by Martin and Unwin[17,18] who extensively studied tip transients in SECM.

These simulations demonstrate that, in considering a quiet time for a specific L and E_S and the subsequent recording of a tip steady-state voltammogram, it is important to select a time where the tip current has reached an apparent quasi-or steady-state regime and where the diffusion-layer thickness well exceeds the distance between the tip and substrate. For example, Figure 5 demonstrates that the choice of a quiet time greater than 2 s could be sufficient for the TCNQ case, with a diffusion-layer thickness of 0.0076 cm compared to 0.012 cm for a 5-s quiet time.

Simulations: TCNQ (Tip Voltammograms). Immediately after the 5-s quiet time, tip voltammograms were computed at specific E_S at a sweep rate of 50 mV/s from $E_T = 0.500$ to 0 V. Figure 6 shows simulations (Femlab) for the $D_{\text{TCNQ}} = D_{\text{TCNQ}^-}$ (solid lines) and $D_{\text{TCNQ}} \neq D_{\text{TCNQ}^-}$ (dashed lines) cases. The tip voltammograms at $E_S = 0.500$ V correspond to the tpf case, which is independent of diffusion coefficient.[17,18] At $E_S = 0$ V, tip voltammograms correspond to the ts case and only anodic tip currents are observed. For $D_{\text{TCNQ}} = D_{\text{TCNQ}^-}$, the magnitude of the anodic limiting tip current is equal but opposite in sign to the limiting cathodic current observed at $E_S = 0.500$ V. For $D_{\text{TCNQ}} \neq D_{\text{TCNQ}^-}$, the anodic limiting current is smaller in magnitude since D_{TCNQ^-} is smaller than in the equal D case and is 3% smaller than the tip current recorded at $E_S = 0.500$ V. At $E_S = E^0 = 0.260$ V, the tip current increases from an anodic limiting current through zero current at $E_T(i_T{=}0) = 0.260$ V, to a cathodic limiting current. For $D_{\text{TCNQ}} = D_{\text{TCNQ}^-}$, the anodic and cathodic limiting currents are equal but opposite in sign and are exactly half the anodic and cathodic limiting current values for the tip voltammograms recorded at $E_S = 0$ and 0.500 V, respectively. For $D_{\text{TCNQ}} \neq D_{\text{TCNQ}^-}$, the anodic limiting current is 6% lower in magnitude than the cathodic limiting current and the ratio of the limiting anodic and cathodic currents to those at $E_S = 0$ and 0.500 V are 2% lower or higher than $^1/_2$, respectively. The half-wave potentials, $E_{T,1/2,}$ are 0.260 and 0.259 V, respectively, for the $D_{\text{TCNQ}} = D_{\text{TCNQ}^-}$ and the $D_{\text{TCNQ}} \neq D_{\text{TCNQ}^-}$ cases.

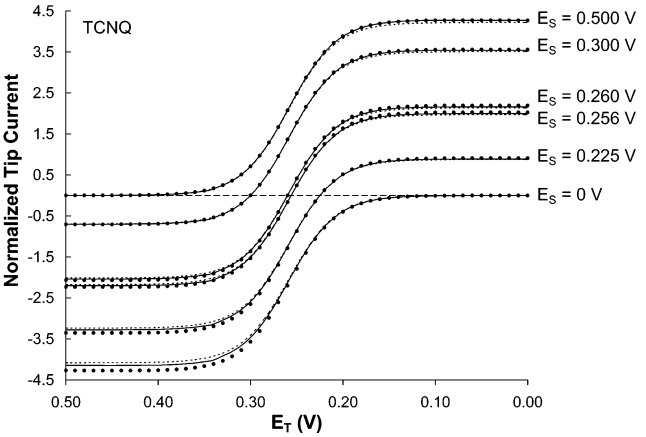

Figure 7. Comparison of quasi-steady-state (solid and dashed lines) and steady-state (solid dots) tip voltammograms for TCNQ when $D_{\text{TCNQ}} = 1.44 \times 10^{-5}$ cm^2/s and $D_{\text{TCNQ}^-} = 1.36 \times 10^{-5}$ cm^2/s (i.e., $D_{\text{TCNQ}}/D_{\text{TCNQ}^-} = 1.06$). Quasi-steady-state (solid lines) and steady-state (solid dots) tip voltammograms performed by Femlab simulations. Quasi-steady-state (dashed lines) tip voltammograms performed by 2D finite difference simulation program. Other simulation parameters as in Figure 2. Long-dashed line indicates zero current.

Steady-state simulations were also carried out for both the $D_{\text{TCNQ}} = D_{\text{TCNQ}^-}$ and the $D_{\text{TCNQ}} \neq D_{\text{TCNQ}^-}$ cases. This involves using a steady-state solver rather than a time-dependent one, so that the quasi-steady-state currents shown in Figure 6 attain true steady-state values. Figure 6 shows that the steady-state tip voltammograms (solid dots) are identical to the corresponding quasi-steady-state tip voltammograms (solid lines) for the $D_{\text{TCNQ}} = D_{\text{TCNQ}^-}$ case. The steady-state tip voltammograms (solid dots) for the $D_{\text{TCNQ}} \neq D_{\text{TCNQ}^-}$ case are shown in Figure 7 along with quasi-steady-state tip voltammograms simulated using both the Femlab simulation program (solid lines) and the 2D finite difference simulation program (dashed lines) written in Fortran in cylindrical coordinates. Figure 7 demonstrates that there is close agreement between the quasi-steady-state tip voltammograms generated using the two different simulation programs. Figure 7 also demonstrates that there are differences between the steady-state and quasi-steady-state tip voltammograms, even in this TCNQ case where there is not a significant difference in D_{TCNQ} and D_{TCNQ^-} (i.e., $D_{\text{TCNQ}}/D_{\text{TCNQ}^-} = 1.06$), as the degree of shielding increases in the tip voltammograms as E_S approaches and moves negative of E^0. From the steady-state tip voltammo-

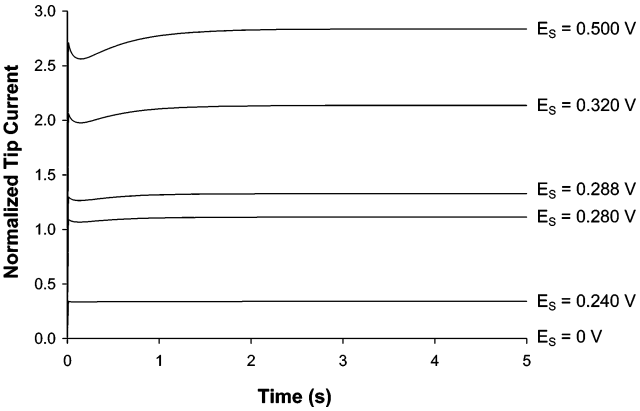

Figure 8. Simulated (Femlab) transient tip response during the 5-s quiet time for ferrocene. The tip potential E_T was held at 0 V at each of the substrate potentials E_S. Other simulation parameters include $L = 0.30$, $E^0 = 0.288$ V, $D_{Fc+} = 1.68 \times 10^{-5}$ cm^2/s, and $D_{Fc} = 2.15 \times 10^{-5}$ cm^2/s (i.e., $D_{Fc+}/D_{Fc} = 0.78$).

grams in Figure 7, one finds that the limiting tip currents at E_S = 0.500 (tpf) and 0 V (ts) are equal in magnitude and opposite in sign. In contrast, from the quasi-steady-state tip voltammogram in Figure 7, the anodic limiting tip current at E_S = 0 V is 3% smaller than the cathodic limiting current at E_S = 0.500 V for this $D_{TCNQ} \neq D_{TCNQ^-}$ case. Since the limiting tip current at E_S = 0.500 V is the same for both the quasi-steady-state and steady-state tip voltammograms, the 3% deviation of the limiting tip current at E_S = 0 V (ts) from that at E_S = 0.500 V (tpf) indicates a 3% deviation from the steady state. Thus, by comparing the magnitudes of the limiting tip currents in experimental tip voltammograms, one can calculate the approximate deviation from steady state. For the experimental tip voltammograms shown in Figure 2, for example, the limiting tip current at E_S = 0 V is 2% smaller than the limiting tip current at E_S = 0.500 V indicating that the quasi-steady-state tip voltammograms are within 2% of the steady state.

Features of both the simulated quasi- and steady-state tip voltammograms for $D_{TCNQ} \neq D_{TCNQ^-}$ include $E_{T,1/2}$ = 0.259 V and $E_T(i_T{=}0) = E_S$ in good agreement with experimental results.

Simulations: Ferrocene (Fc$^+$/Fc) (Quiet Time). The ferrocene system represents a reversible redox mediator with significantly different diffusion coefficients, compared to TCNQ. We used diffusion coefficients of $D_{Fc+} = 1.68 \times 10^{-5}$ cm^2/s and $D_{Fc} = 2.15 \times 10^{-5}$ cm^2/s (i.e., $D_{Fc+}/ D_{Fc} = 0.78$) and a standard potential E^0 = 0.288 V in all simulations found from best fits of the experimental tip voltammograms. As in the TCNQ case, we looked at the tip response during a 5-s quiet time as well as during the following linear potential sweep. Figure 8 shows the normalized tip current versus time response for a UME tip positioned at $L = 0.3$ above an infinite substrate, with E_T = 0 V and E_S ranging from 0 to 0.500 V. When $E_T = E_S$ = 0 V, there is no reaction at either the tip or substrate, and the normalized tip current is 0 throughout the quiet time. As E_S increases, a cathodic tip current flows in response to the Fc$^+$ generated in the tip−substrate gap and across the substrate surface. As with the TCNQ system, this tip current is initially transient in nature in that there is an instantaneous cathodic value as the Fc$^+$ generated at the substrate reaches the tip followed by a brief decay and then an increase in the cathodic current toward a quasi-steady value as the Fc$^+$ diffusion layer is established across the substrate and in the tip−substrate gap and positive feedback begins. The transient nature of the tip current depends on L, D_{Fc}, D_{Fc+}, and E_S and is most apparent when E_S is in the vicinity of and at values more positive than E^0. Comparison with Figure 5a for the TCNQ system where D_{TCNQ}/D_{TCNQ-} = 1.06 demonstrates the effect that the diffusion coefficient ratio has on the quiet time i_T versus t curves and is in agreement with transient results reported by Martin and Unwin.[17,18] Figure 8 shows that a minimum quiet time (≈ 3−4 s) somewhat longer than that for the TCNQ case (≈ 2 s, from Figure 5) is necessary with very different diffusion coefficients to establish a quasi-steady tip current.

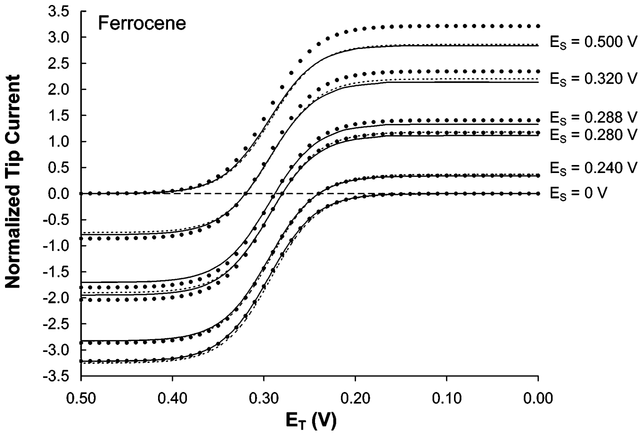

Figure 9. Comparison of quasi-steady-state (solid and dashed lines) and steady-state (solid dots) tip voltammograms for ferrocene. Quasi-steady-state (solid lines) and steady-state (solid dots) tip voltammograms calculated by Femlab simulations. Quasi-steady-state (dashed lines) tip voltammograms calculated by 2D finite difference simulation program. Simulation parameters as in Figure 3. Long-dashed line indicates zero current.

Simulations: Ferrocene (Fc$^+$/Fc) (Tip Voltammograms). Immediately after the 5-s quiet time, tip voltammograms were recorded at a sweep rate of 50 mV/s from E_T = 0 to 0.500 V in response to the underlying substrate held at values of E_S over the same potential range. Figure 9 shows both transient (Femlab, solid line; finite difference program, dashed lines) and steady-state (Femlab, solid dots) simulations. Again, there is good agreement between the quasi-steady-state tip voltammograms generated using the two different simulation programs. The tip voltammograms at E_S = 0 V correspond to the tpf case, which is independent of diffusion coefficients. Moreover, in this case, the transient simulations and steady-state simulations give identical normalized tip voltammograms. At E_S = 0.500 V (ts), tip voltammograms with only cathodic limiting currents are observed. The normalized tip current from the transient simulation is 12% smaller than that at E_S = 0 V since $D_{Fc+} < D_{Fc}$. This suggests a 12% deviation from the steady state with the L, D, and E_S parameters reported, a difference that is verified by the normalized steady-state tip voltammogram (solid dots), which is identical to that simulated at E_S = 0 V. For the experimental tip voltammograms shown in Figure 3, the limiting tip current at E_S = 0.500 V is also 12% smaller than the limiting tip current at E_S = 0 V, indicating that the quasi-steady-state tip voltammograms are within 12% of the steady state. At $E_S = E^0$ = 0.288 V, the tip current decreases from a cathodic limiting current through zero current at $E_T(i_T{=}0)$ = 0.288 V, to an anodic limiting current. The ratio of the anodic and cathodic limiting currents is approximately $^1/_2$ for both the quasi- and steady-state voltammograms. The $E_{T,1/2}$ values were 0.294 V for both the quasi-steady-state and steady-state tip voltammograms and E_T (i_T=0) = E_S, in good agreement with values determined from the experimental tip voltammograms.

Approximate Quasi-Steady-State Equations. In this section, we report approximate equations to describe the quasi-steady-state voltammograms shown by the preceding experiments and simulations. The derivations are reported in the Supporting Information. When only species O is initially present in solution, the quasi-steady-state current is

$$I_T(E_T,E_S,L) = \frac{i_T(E_T,E_S,L)}{i_{T,\infty}^{\lim,c}} = \frac{\xi(\theta_S - \theta_T)f_T(L)}{(1+\xi^2\theta_T)(1+\xi\theta_S)} \tag{6}$$

and when only species R is initially present in solution

$$I_T(E_T,E_S,L) = \frac{i_T(E_T,E_S,L)}{|i_{T,\infty}^{\lim,a}|} = \frac{\xi^2(\theta_S - \theta_T)f_T(L)}{(1+\xi^2\theta_T)(1+\xi\theta_S)} \tag{7}$$

where $\xi = (D_O/D_R)^{1/2}$ and θ_S and θ_T are the surface concentration ratios given by equation SIA-1 when $E = E_S$ or $E = E_T$, respectively. Comparison between the quasi-steady-state tip voltammograms generated using the approximate eqs 6 and 7 (dashed lines) shows excellent agreement with those generated from the Femlab transient simulations (solid lines) in Figure S1 for the TCNQ redox mediator and Figure S2 for the ferrocene mediator in the Supporting Information. Equations 6 and 7 permit relationships to be established for the limiting currents of each tip voltammogram and the ratios between limiting currents, which are in excellent agreement (≤0.3% difference) with those found from corresponding tip voltammograms generated from Femlab transient simulations (solid line) for $L \le 0.3$ and $D_O/D_R \ge 0.78$; the approximate equations have not been tested extensively outside of these parameters.

When only species O is in solution, the following limits result from eq 6. For quasi-steady-state tip voltammograms in the tpf and ts limits

tpf ($E_T = -\infty$, $E_S = \infty$, $L \le 0.3$):

$$I_{T,\lim,c}^{tpf} = f_T(L)$$

ts ($E_T = -\infty$, $E_S = \infty$, $L \le 0.3$): (8)

$$I_{T,\lim,a}^{ts} = \frac{-f_T(L)}{\xi} \tag{9}$$

The ratio of eqs 8 and 9

$$\frac{I_{T,\lim,c}^{tpf}}{|I_{T,\lim,a}^{ts}|} = \xi = \sqrt{D_O/D_R} \tag{10}$$

permits the determination of the D_O/D_R ratio directly from experimental data; knowing D_O from $i_{T,\infty}^{\lim,c}$ (eq 3) allows D_R to be calculated. From quasi-steady-state tip voltammograms in the pf-ps limits

pf-ps ($E_T = \pm\infty$, finite E_S, and $L \le 0.3$):

$$I_{T,\lim,c}^{pf-ps}(E_T = -\infty,E_S,L) = \frac{\theta_S \xi f_T(L)}{1+\xi\theta_S} \tag{11}$$

$$I_{T,\lim,a}^{pf-ps}(E_T = \infty,E_S,L) = \frac{-f_T(L)}{\xi(1+\xi\theta_S)} \tag{12}$$

The ratio of (11) and (12)

$$\frac{I_{T,\lim,c}^{pf-ps}(E_T = -\infty,E_S,L)}{|I_{T,\lim,a}^{pf-ps}(E_T = \infty,E_S,L)|} = \xi^2\theta_S \tag{13}$$

allows the magnitudes of the limiting cathodic and anodic branches of the pf-ps quasi-steady-state tip voltammograms to be compared quantitatively and also facilitates the calculation of E^0 (i.e., $\theta_S = 1$, when $E_S = E^0$) by rearrangement of eq 13

$$E^0 = E_S - \frac{RT}{nF} ln\left\{\frac{D_R}{D_O}\frac{I_{T,\lim,c}^{pf-ps}(E_T = -\infty,E_S,L)}{|I_{T,\lim,a}^{pf-ps}(E_T = \infty,E_S,L)|}\right\} \tag{14}$$

The half-wave potential $E_{1/2}$ can then be calculated according to

$$E_{1/2} = E^0 - \frac{RT}{nF} ln\left\{\frac{D_O}{D_R}\right\} \tag{15}$$

The magnitude of the limiting pf-ps tip currents relative to the limiting tpf and ts conditions is as follows:

$$\frac{I_{T,\lim,c}^{pf-ps}(E_T = -\infty,E_S,L)}{I_{T,\lim,c}^{tpf}(E_T = -\infty,E_S = \infty,L)} = \frac{\xi\theta_S}{1+\xi\theta_S} \tag{16}$$

$$\frac{I_{T,\lim,a}^{pf-ps}(E_T = \infty,E_S,L)}{I_{T,\lim,c}^{ts}(E_T = \infty,E_S = -\infty,L)} = \frac{1}{1+\xi\theta_S} \tag{17}$$

Thus, at $E_S = E^0$ (i.e., $\theta_S = 1$) and equal diffusion coefficients ($\xi = 1$), for example, the ratio is exactly 1/2, as the simulations demonstrated.

These limiting tip currents and tip current ratios given by eqs 8−17 for only species O initially in the bulk solution provide diagnostic criteria for looking at a family of quasi-steady-state tip voltammograms if the diffusion coefficient ratio and E^0 are known for a redox couple and a means for calculating them if they are not. Thus, for the experimental tip voltammograms shown in Figure 2 for the TCNQ mediator, one finds from eq 10 that the limiting currents are not equal, indicating that the tip voltammograms are quasi-steady-state and within 2% of the steady state. From the eq 10 ratio, $D_{TCNQ}/D_{TCNQ^-} = 1.04$ is found from the limiting currents shown in Figure 2 and is in close agreement with the 1.06 value found from Femlab transient simulation fittings of these experimental quasi-steady-state tip voltammograms. Similarly, from eqs 14 and 15, one finds $E^0 = E_{1/2} = 259$ mV ± 2 mV in good agreement with the simulation value of 260 mV and an experimental $E_{1/2} = 257$ mV ± 2 mV measured directly from the tip voltammograms. Additionally, one can look at the relative changes in the quasi-steady-state tip voltammograms via eqs 16 and 17 and find agreement within ±4% from one tip voltammogram to the next. A final diagnostic criterion is that the tip potential E_T at which the tip current crosses zero is equal to the substrate potential E_S that was used in generating the concentration profiles; thus, $E_T(i_T{=}0) = E_S$, as predicted by eq 6; this relationship is true irrespective of the diffusion coefficient ratio. For the quasi-steady-state tip voltammograms shown in Figure 2, $E_T(i_T{=}0) = E_S \pm 2$ mV was found.

Similar relationships based on eq 7 in which only species R is initially present in the bulk solution follow similar arguments. For quasi-steady-state tip voltammograms in the tpf and ts limits

tpf ($E_T = \infty$, $E_S = -\infty$, $L \le 0.3$):

$$I^{\text{tpf}}_{\text{T,lim},a} = -f_T(L) \tag{18}$$

ts ($E_T = -\infty$, $E_S = \infty$, $L \le 0.3$):

$$I^{\text{ts}}_{\text{T,lim},c} = \xi f_T(L) \tag{19}$$

From the ratio of eqs 18 and 19

$$\frac{I^{\text{ts}}_{\text{T,lim},c}}{|I^{\text{tpf}}_{\text{T,lim},a}|} = \xi = \sqrt{D_O/D_R} \tag{20}$$

the D_O/D_R ratio can be found, and knowing D_R from $i^{\text{lim},a}_{\text{T},\infty}$, allows D_O to be calculated.

For pf-ps quasi-steady-state-tip voltammograms

pf-ps ($E_T = \pm\infty$, finite E_S, and $L \le 0.3$):

$$I^{\text{pf-ps}}_{\text{T,lim},c}(E_T = -\infty, E_S, L) = \frac{\xi^2 \theta_S f_T(L)}{1 + \xi\theta_S} \tag{21}$$

$$I^{\text{pf-ps}}_{\text{T,lim},a}(E_T = \infty, E_S, L) = \frac{-f_T(L)}{1 + \xi\theta_S} \tag{22}$$

The ratio of eqs 21 and 22 is identical to eq 13; allows the magnitudes of the limiting cathodic and anodic branches of the quasi-steady-state tip voltammograms to be compared quantitatively; and facilitates the calculation of E^0 and $E_{1/2}$ according to eqs 14 and 15. The magnitude of the limiting quasi-steady-state tip currents given by eqs 21 and 22 relative to the tpf (eq 18) and ts (eq 19) limits are identical to eqs 16 and 17. These limiting tip currents and tip current ratios derived from eq 7 for only species R initially in the bulk solution provide diagnostic criteria for looking at a family of tip voltammograms as was done for the preceding TCNQ case. A final diagnostic criterion is that the tip potential E_T at which the tip current crosses zero is equal to the substrate potential E_S that was used in generating the concentration profiles; thus, $E_T(i_T{=}0) = E_S$, as predicted by eq 7, independent of the diffusion coefficient ratio. Thus, for the experimental tip voltammograms shown in Figure 3 for the ferrocene mediator, one finds from eq 20 that the limiting currents are not equal, indicating that the tip voltammograms are quasi-steady-state and within 12% of the steady state. From the eq 20 ratio, $D_{\text{Fc+}}/D_{\text{Fc}} = 0.77$ is found from the limiting currents shown in Figure 3 and is in good agreement with the 0.78 value found from Femlab transient simulation fittings of these experimental quasi-steady-state tip voltammograms. Similarly, from eqs 14 and 15 one finds $E^0 = 286 \pm 2$ mV and $E_{1/2} = 293 \pm 2$ mV in good agreement with the transient Femlab simulation value of $E^0 = 288$ mV and an experimental $E_{1/2} = 294 \pm 3$ mV. Additionally, one can look at the relative changes in the experimental quasi-steady-state tip voltammograms via eqs 16 and 17 and find agreement within ±10% from one tip voltammogram to the next. Finally, for the quasi-steady-state tip voltammograms shown in Figure 3, $E_T(i_T{=}0) = E_S \pm 3$ mV was found.

Approximate Steady-State Equations. Following from the Supporting Information, an approximate steady-state equation for species O or R initially present in the bulk solution is

$$I_T(E_T,E_S,L) = \frac{i_T(E_T,E_S,L)}{i^{\text{lim},c}_{\text{T},\infty}} = \left|\frac{i_T(E_T,E_S,L)}{i^{\text{lim},a}_{\text{T},\infty}}\right| = \frac{\xi^2(\theta_S - \theta_T) f_T(L)}{(1 + \xi^2\theta_T)(1 + \xi^2\theta_S)} \tag{23}$$

The tip voltammograms from this approximate steady-state expression (dashed line) show good agreement (within ±0.3%) with the simulated steady-state tip voltammograms (Femlab) (solid dots) in Figure S1 for TCNQ and Figure S2 for ferrocene. In the tpf and ts limits, eq 23 predicts that for species O initially in solution

$$I^{\text{tpf}}_{\text{T,lim},c} = f_T(L) \tag{24}$$

$$I^{\text{ts}}_{\text{T,lim},a} = -f_T(L) \tag{25}$$

$$\frac{I^{\text{tpf}}_{\text{T,lim},c}}{|I^{\text{ts}}_{\text{T,lim},a}|} = 1.000 \tag{26}$$

for any diffusion coefficient ratio. Thus, the limiting currents under total feedback and extreme shielding are equal but opposite in sign, as found in the steady-state simulations (Femlab). A similar argument follows for the case where only R is initially present in solution.

CONCLUSIONS

SECM experiments deal with a number of variables (E_T, E_S, i_T, i_S, L...) and provide large amounts of data that can be usefully obtained and represented in different ways, e.g., approach curves, tip and substrate voltammograms in generation/collection experiments.[1−3] We have discussed here the usefulness of tip voltammograms under quasi-steady-state and steady-state conditions. The features of tip voltammograms in this mode depend upon the distance d between a UME tip and an underlying substrate, the potential E_S of the substrate relative to E^0 of the redox mediator in the bulk solution, the quiet time τ before sweeping the tip potential E_T, and the diffusion coefficient ratio of diffusing redox species contributing to the tip current. When

E_S is held at a value where the substrate and tip are performing the same reaction (i.e., O + ne $\leftrightarrows$ R, for a reduction), the tip becomes shielded by the substrate from the bulk solution. For reversible reactions, this means that the tip is immersed in a layer of O and substrate-generated R and the tip voltammogram is composed of both anodic (corresponding to R) and cathodic (corresponding to O) contributions to the tip current as E_T is swept between positive and negative limits. The degree of shielding of each tip voltammogram is evident in the anodic offset of the entire tip voltammogram from that where no shielding occurs (i.e., extreme positive potentials relative to E^0) due to the substrate reaction. Positive feedback also occurs in such shielded tip voltammograms at positive E_T due to substrate-generated R and at negative E_T due to species O in the bulk solution.

For large substrates relative to the UME tip, the tip−substrate distance d, the quiet time τ, and diffusion coefficient ratio determine whether the tip voltammograms will be quasi-steady-state or steady state. The tip−substrate distance should be less than a tip radius, and the quiet time should be sufficiently large that the diffusion layer of electrogenerated species is large compared to the tip−substrate separation and the tip current is constant. Under these conditions, if $D_O = D_R$, then the diffusion layer quickly reaches a steady state and a steady-state tip voltammogram is recorded. If $D_O \neq D_R$, then the diffusion layer generally remains a function of time and a quasi-steady-state tip voltammogram is recorded. Transient simulations showed good agreement with experimental quasi-steady-state tip voltammograms for the TCNQ system where $D_{TCNQ}/D_{TCNQ^-} = 1.06$ and ferrocene where $D_{Fc+}/D_{Fc} = 0.78$. Steady-state simulations were also performed and permitted a comparison between steady-state and quasi-steady-state tip voltammograms. Approximate equations were developed to permit definitive descriptions of the features of both steady-state and quasi-steady-state tip voltammograms; these approximate equations showed good agreement (<0.3%) with results of the simulations.

Shielding experiments of the type described here have several advantages. First, it is possible to obtain information about redox species that can only be electrogenerated. For example, by electrogenerating R at the substrate from O in the bulk solution and creating a sufficiently thick diffusion layer of R around the tip−substrate gap, the tip responds as if R was now the bulk concentration species and the resulting tip voltammogram leads to information about D_R and heterogeneous kinetics of the O/R couple. Second, if electrogenerated R is unstable in solution, information about D_R and homogeneous kinetics can be obtained by varying the tip−substrate distance. Third, as demonstrated in this report, one can obtain information about the D_O/D_R ratio by recording a series of shielding tip voltammograms at one tip−substrate distance. Such information is not available from cyclic voltammograms at large electrodes or steady-state voltammograms at small electrodes unless one does bulk electrolysis of species O. RRDE experiments[23] could also be used, but one would first need to determine the collection efficiency (dependent on the gap between the disk and surrounding ring) of the RRDE assembly and the theory for such experiments is significantly more complicated than for SECM. In principle, thin-layer cells could be run similar to the SECM arrangement with differing potentials on the electrodes which form the thin-layer cells. However, in reality, this is difficult to achieve because the combination of large electrodes and a small gap leads to a large resistance, which distorts the voltammograms due to the iR drop across the cell.[24] Interdigitated electrodes could also be used in experiments similar to SECM, but these are microfabricated devices with fixed widths between facing electrodes and several such devices with varying interelectrode spacings would be required to perform the equivalent of SECM experiments. Thus, SECM has advantages over other electrochemical methods in the shielding experiments described here of high mass transport to the UME tip, small iR drops, interelectrode spacing that can be readily changed, and simpler theories to describe the resulting tip voltammograms.

ACKNOWLEDGMENT

The support of this work by grants from the National Science Foundation (C.G.Z. CHE-0210315, EPS-0447691/NMSU Cost-share, ADVANCE; A.J.B. CHE-0451494) are acknowledged. C.R.L. acknowledges funding from the American Chemical Society Petroleum Research Fund (PRF-41607).

SUPPORTING INFORMATION AVAILABLE

Figures related to tip voltammograms using approximate quasi- and steady-state equations, description of the Femlab model, and description of the finite difference simulation. This material is available free of charge via the Internet at http://pubs.acs.org.

Received for review January 3, 2007. Accepted April 10, 2007.

AC070021C

---

[23] Reference 5, Chapter 9.

[24] Goldberg, I. B.; Bard, A. J. *J. Electroanal. Chem.* **1972**, *38*, 313.